Avoiding RF Isolators: Reflectionless Microwave Bandpass Filtering Components for Advanced RF Front Ends

Article *in* IEEE Microwave Magazine · December 2020

DOI: 10.1109/MMM.2020.3023222

CITATION
1

READS
87

4 authors, including:

Dimitra Psychogiou
Purdue University
155 PUBLICATIONS **1,092** CITATIONS
SEE PROFILE

Li Yang
University of Alcalá
49 PUBLICATIONS **287** CITATIONS
SEE PROFILE

Avoiding RF Isolators

Roberto Gómez-García, Dimitra Psychogiou, José-María Muñoz-Ferreras, and Li Yang

RF/microwave bandpass filters (BPFs) are fundamental components in high-frequency RF transceivers. On the transmitter side, they limit the transmitted RF signal bandwidth by suppressing out-of-band spurious signals and intermodulation products, which are primarily generated by the nonlinear active stages and can affect other RF systems. On the other hand, in the receiver, they reject out-of-band interfering/jamming signals and noise. Whereas a large variety of microwave BPFs have been proposed in the technical literature for multiple technologies (e.g., [1] and [2]), most of these BPF devices achieve their filtering functionality by means of the frequency-selective power reflection processing of the RF input signal. This means that those RF signals allocated within the operational bandwidth of the BPF are transmitted to the output terminal (with some tolerable added in-band loss and

Roberto Gómez-García (roberto.gomez.garcia@ieee.org), José-María Muñoz-Ferreras (jm.munoz@uah.es), and Li Yang (li.yang@uah.es) are with the Department of Signal Theory and Communications, University of Alcalá, Spain. Dimitra Psychogiou (dimitra.psychogiou@colorado.edu) is with the Department of Electrical, Computer, and Energy Engineering, University of Colorado Boulder.

Digital Object Identifier 10.1109/MMM.2020.3023222
Date of current version: 6 November 2020

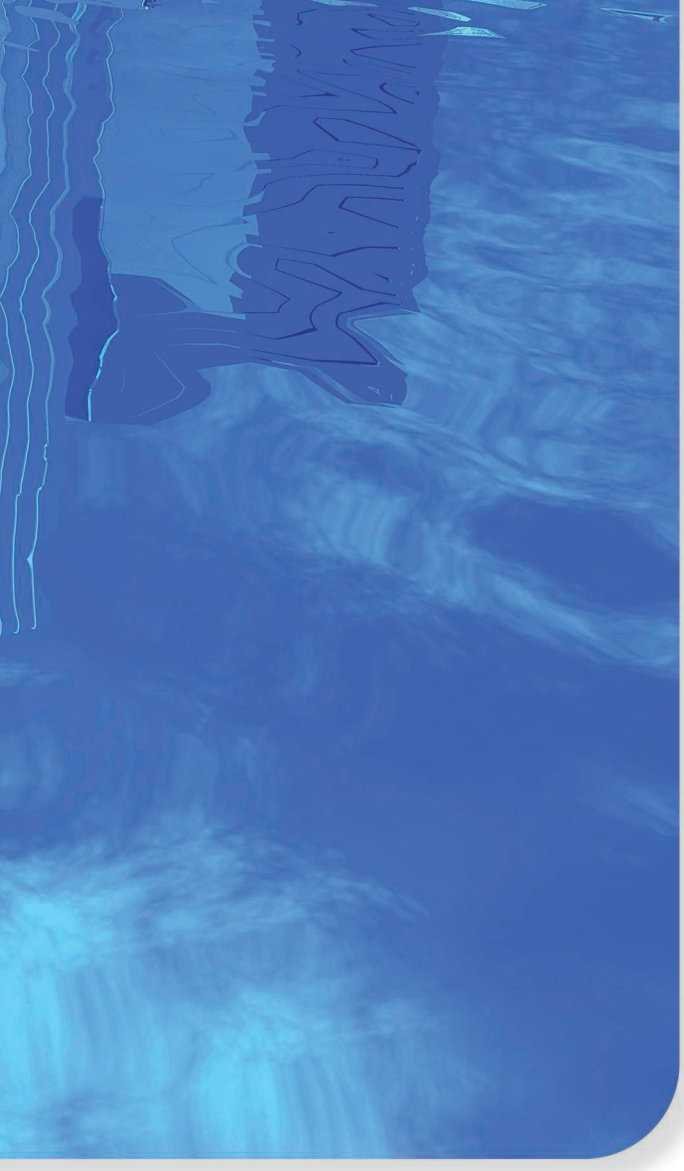

©SHUTTERSTOCK/JOINGATE

amplitude/phase distortion), whereas the ones present in the BPF stopband regions are reflected back at the input terminal.

Nevertheless, such undesired out-of-band RF signal energy reflections can lead to adverse consequences in the RF operation of neighboring active components, such as frequency conversion stages and amplifying blocks [3], [4]. For example, the stopband RF signal power reflections associated with the intermodulation products and local oscillator (LO) harmonics coming back from a reflective-type BPF placed just after a mixer can produce additional spurious signals. This is due to their remixing with the desired signals in an iterative process that may fall within the operational bandwidth, as illustrated in Figure 1(a) (i.e., intermodulation expansion), which results in a reduction in the dynamic range of the overall RF system. Besides, as shown in Figure 1(b), they can create standing waves in the interconnection transmission lines between the mixer and the reflective-type filter, hence decreasing the mixer conversion gain.

Furthermore, these unwanted RF signal power echoes can induce RF amplifiers to become unstable and create aliased harmonics in analog-to-digital converters, thus hindering their operation. All these negative effects can lead to the complete malfunction of the entire RF front-end chain so that their efficient mitigation becomes mandatory. This issue becomes even more important when one considers the large number of active components that can be found in today's multipurpose/service RF transceiver modules, which are capable of supporting multiple standards at the same time [5].

Traditionally, the mitigation of RF power reflection in RF transceivers has been accomplished through different strategies, all of which show some deficiencies. The most commonly adopted solution involves the use of an RF isolator inserted between the active element and the reflective-type BPF so that the out-of-band RF signal power reflections coming from the BPF do not reach the active stage. However, passive magnetic/ferrite-based isolators are bulky and difficult to integrate, whereas isolators using nonreciprocal active elements (e.g., transistors) consume extra dc power [6]. Attenuator stages can also be employed, but they introduce a significant loss in the direct/forward path, which degrades the signal-to-noise ratio and needs to be compensated for with additional amplifier blocks so that the extra dc power issue is reinstated. As a third option, interference cancellation schemes (e.g., circulator-, multistage duplexer-, and feedforward reflection-based approaches) may be employed [7]. However, depending on the type, they suffer from being bulky and sensitive in their operation and also exhibiting a narrowband behavior. Thus, none of these RF power reflection suppression methods seems to offer an effective solution to the problem.

A more efficient procedure to eliminate unwanted out-of-band RF signal power reflections may be the exploitation of reflectionless, or absorptive, microwave BPFs as replacements for their classical reflective-type counterparts. Reflectionless BPFs are lossy filtering circuits that, inside themselves, dissipate the nontransmitted out-of-band RF input signal energy instead of reflecting it back to the source [8]. As a result, the problem of RF signal power echo generation in RF transceivers can be overcome without additional circuitry, as detailed in Figure 1(b).

The purpose of this overview article is to provide a complete summary of the main design techniques and state-of-the-art RF components in the field of reflectionless BPF devices. It should be remarked that, whereas a rich number of solutions for absorptive bandstop filter (BSF) components and applications (e.g., multiharmonic absorption circuits to increase efficiency in power amplifiers and RF reflectionless negative group

delay processors) have been reported [9]–[22], fewer efforts have been carried out for the development of reflectionless BPFs. This is due to the greater difficulty inherent in the design of reflectionless BPFs, where the RF power absorption process must be accomplished in at least two noncontiguous frequency intervals (i.e., the lower and upper stopbands) without significantly affecting the in-band performance.

Reflectionless BPFs: Design Techniques and Planar Prototypes

As described in the previous section, reflectionless/absorptive BPFs consume within their circuit volume the nontransmitted RF input signal energy in the stopband ranges of their transfer function instead of returning it to the source, meaning that no RF signal power echoes are created. As such, these types of BPFs must have lossy elements in their circuit networks (i.e., lumped resistors and/or resistive materials) so that RF signal energy consumption can be dissipated as heat [23]. Note that, in this article, other mechanisms of loss, such as RF signal radiation, are not contemplated. Hence, sharing this philosophy as a common background, different types of RF design techniques for reflectionless BPF devices have been reported in the technical literature. A summary of these design methods, including a description of their benefits and limitations as well as a discussion of practical examples of proof-of-concept planar prototypes, is provided in the following.

- *Complementary diplexer-based BPFs [24]–[28]*: These two-channel diplexing architectures are composed of a "main" bandpass-type channel and an "auxiliary" bandstop-type channel whose transfer

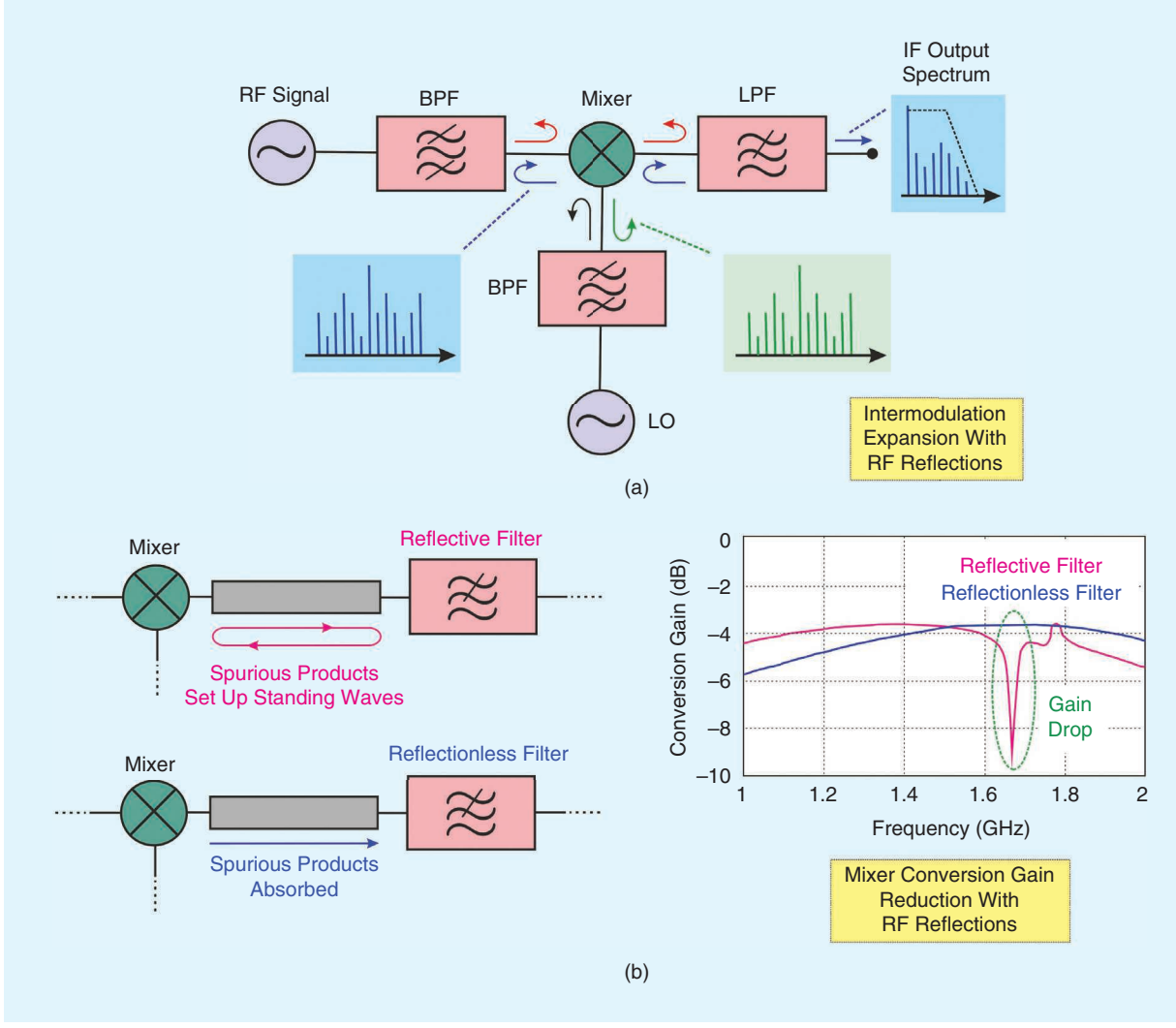

Figure 1. *The problems of (a) intermodulation expansion in a receiver's low-conversion stage due to multiple out-of-band RF signal power reflections produced by reflective-type filters and (b) mixer conversion gain reduction resulting from generated standing waves in interconnection transmission lines [3]. LPF: low-pass filter; IF: intermediate frequency.*

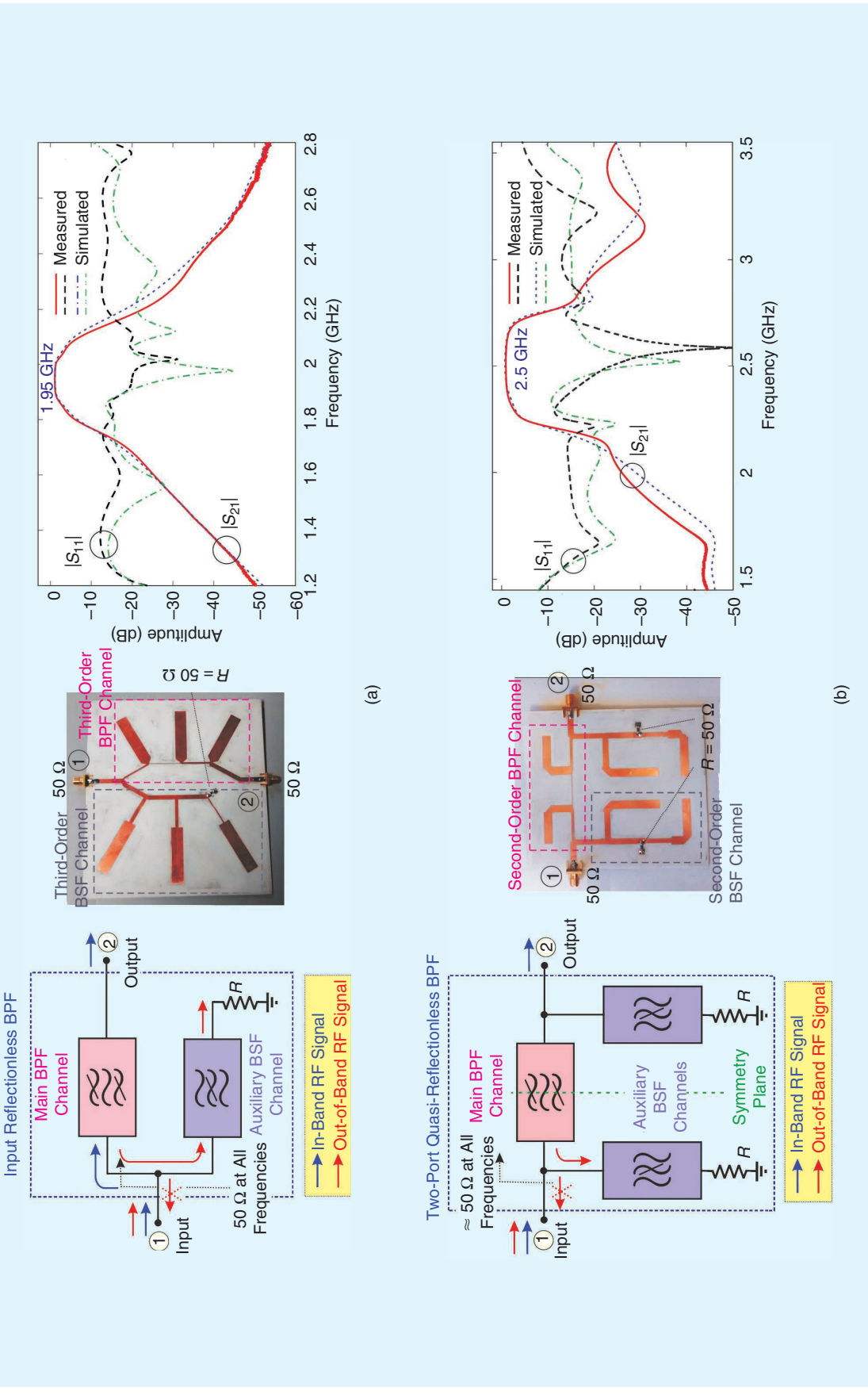

Figure 2. *Examples of reflectionless BPFs in microstrip technology based on complementary diplexer architectures along with their measured and simulated results. (a) An input reflectionless BPF [25]. (b) A two-port quasi-reflectionless BPF [26].*

functions are complementary or opposite in frequency (i.e., interchannel input susceptance compensation) [24], [25]. The main bandpass channel is connected between the input and output terminals of the overall filter so that it determines the in-band characteristics of the entire filtering device by enabling RF signal transmission in its passband range.

The auxiliary bandstop channel is connected at the overall input terminal and ended in a loading resistor at its other access. In this manner, the RF signal energy reflected at the input of the main channel in its stopband regions is dissipated in the loading resistor of the auxiliary channel instead of being reflected back to the source. This enables input reflectionless capabilities to be attained in the overall BPF network by virtually presenting an input impedance equal to the reference impedance at any frequency for an overall bandpass behavior. It should be noted that the complementary diplexer concept can be extended to two-port/symmetrical realizations by loading the auxiliary absorptive bandstop branch at the two filter terminals. However, this is done at the expense of passing from a theoretically perfect reflectionless behavior to a quasi-reflectionless one and at the cost of a higher influence of the absorptive component on the in-band behavior in terms of amplitude rounding at the passband edges [26], [27].

The advantages of this class of reflectionless BPF design techniques include the availability of analytical/semianalytical coupling-routing-diagram-based and polynomial-synthesis techniques for bandpass transfer functions with/without transmission zeros (TZs) and the avoidance of signal transmission cross paths between the reflective/reactive BPF and absorptive/lossy BSF sections that could make the total BPF design more sensitive. The approaches' major drawback is a large circuit size for high-order implementations. Note also that the limited reflectionless bandwidth resulting from the frequency-dependence profile of the impedance inverters when implemented as quarter-wavelength transmission line sections can be pointed out as an additional shortcoming.

However, some developments based on multimode resonators and defected ground structures have been proposed to enhance this figure of merit [28]. For illustration purposes, Figure 2 presents the RF operational principle and the results of two proof-of-concept microstrip prototypes corresponding to one- and two-port reflectionless planar BPFs with third- and second-order transfer functions centered at 1.95 and 2.5 GHz, respectively [25], [26]. They feature 10-dB referred reflectionless bandwidth ranges of 1.09–2.83 GHz for the input reflectionless BPF (i.e., 7.3 times its 239-MHz, 3-dB passband width) and of 1.49–3.36 GHz for the two-port quasi-reflectionless BPF (4.3 times its 455-MHz, 3-dB passband width).

- *Lossy-stub-based BPFs [29]–[32]*: These devices make use of absorptive networks connected at the input or at both terminals of a reflective-type BPF that is placed at the direct input-to-output signal path to attain input or two-port reflectionless behavior, respectively. These lossy networks are shaped by a resistor followed by a reactive circuit network (i.e., a stub in the transmission line case, as in [29], [31], and [32]), which becomes an inductor–capacitor network, as in [30], for lumped element implementations. In the passband region, the aforementioned reactive network ideally must exhibit an open circuit at its input so that the effect of its dissipative resistor in that frequency region becomes transparent. However, in the out-of-band region, the reactive network input impedance preferably should be a short circuit so that the resistor can absorb the RF signal energy reflected by the reflective-type BPF component in its stopband regions.

Compared to the complementary diplexer approach, the advantages of this technique are increased simplicity and a smaller size in high-order BPF realizations. Nevertheless, its main drawback is the more perceptible influence of the lossy stubs in the passband region of the overall reflectionless BPF, with a significant passband amplitude rounding effect that means there is more amplitude distortion across in-band processed signals [29]–[31]. This can be counteracted by using higher-order reactive networks to better compensate for the response of the reflective-type BPF component, although the size limitation issue is reinstated [9].

Figure 3 depicts the circuit detail and results of a proof-of-concept, three-stage microstrip prototype of a 1.6-GHz wideband reflectionless BPF based on this approach, which uses transversal signal interference filtering sections as constituent reflective-type filtering parts [32] (note that stub-loaded-based and coupled-line BPF topologies are used instead, in [29] and [31], respectively). As can be seen, it features a 10-dB-referred input reflectionless bandwidth from 0.754 to 2.565 GHz as the main performance metric (i.e., 7.3 times the 3-dB transmission bandwidth of 248 MHz).

- *Balanced-circuit-based BPFs [33], [34]*: These exploit a two-channel balanced circuit made up of two similar wideband 3-dB quadrature couplers at the input and output sides and two identical reflective-type BPFs. Specifically, as shown in Figure 4, these BPFs are separately connected in each branch between the direct and coupler ports of the couplers and determine the overall transfer function of the reflectionless BPF. By means of the balanced structure, the out-of-band RF signal power reflections coming from the reflective-type BPFs are absorbed in the reference impedance resistors that load the isolated ports of the couplers so that symmetrical reflectionless characteristics are obtained [33].

  In practice, the main shortcomings of this procedure are found in the operational bandwidth of the wideband 3-dB quadrature couplers, which limits the reflectionless bandwidth of the entire BPF structure and makes the arrangement's application to reconfigurable designs very challenging. Furthermore, a proper pairing of the reflective-type BPFs embodied in each branch and low amplitude/phase imbalances for the wideband 3-dB quadrature couplers are essential factors to ensure good reflectionless behavior in the total BPF device [34].
- *Symmetrical BPFs with even/odd-mode subcircuit compensation [35]–[37]*: These correspond to symmetrical and lossy electrical networks in which the even- and odd-mode circuit subnetworks exhibit opposite input reflection coefficients (i.e., $\Gamma_{even} = -\Gamma_{odd}$) as a design goal to attain perfect two-port absorptive behavior at their two accesses. Note that the achievement of such a condition generally requires circuit structures with several signal propagation paths between the input and output terminals. One example of such an approach for a transmission line realization was reported in [35] [Figure 5(a)], showing a sharp-rejection bandpass transfer function with close-to-passband TZs and fully reflectionless behavior.

  However, the positions of the TZs in the reflectionless BPF cell are not flexible since they are determined by the intended 3-dB passband width. Inspired by this design method, a more general approach facilitating the realization of more arbitrary filtering responses was proposed in [37] [Figure 5(b)] and verified with lumped element demonstrators, although it could be applied to transmission line schemes. Note that this procedure has as its major advantage the realization of quasi-elliptic-type BPFs with two-port, fully absorptive behavior despite the presence of

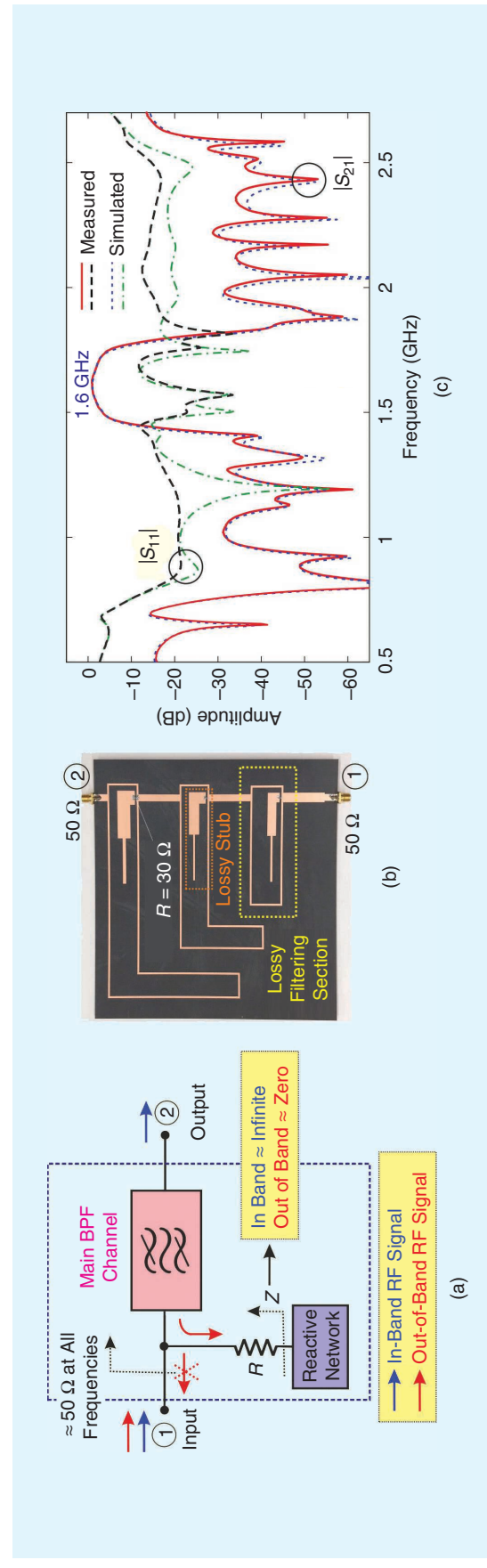

Figure 3. *An example of (a) an input quasi-reflectionless BPF in microstrip technology using (b) lossy transversal signal interference-filtering sections with input lossy stubs [32]. (c) The measurement and simulated results.*

several signal propagation paths, which makes them sensitive to manufacturing tolerances.

Finally, it must be highlighted that, in some cases, the previous categories of RF design techniques for reflectionless BPFs can be viewed as interoverlapped procedures. For example, the auxiliary, resistively terminated bandstop channel in the complementary diplexer approach may also be considered a lossy stub, in which case the resistor is placed at the output terminal instead of at the input node. Moreover, the balanced circuit-based reflectionless BPF architecture also shows theoretically perfect mutual cancellation in terms of the input reflection coefficients between its even- and odd-mode subcircuit networks as a fundamental condition to attain the two-port absorptive behavior.

Beyond Static, Reflectionless, Planar, Single-Band BPFs

The RF design techniques discussed in the preceding for microwave reflectionless BPF realization in planar technologies can be extended to more sophisticated RF passive devices, leading to completely new families of high-frequency absorptive BPF components. In addition, other nonplanar technologies can benefit from RF reflectionless principles in which the generation of undesired RF signal power reflections can become even more critical due either to the presence of more active elements in the RF front-end chain [as in monolithic microwave integrated circuit (MMIC) transceivers] or to the handling of higher RF signal power levels (as in satellite communication RF modules). This section provides a summary of more advanced reflectionless microwave BPF devices, including multiband, spectrally adaptive, and multifunctional components. Furthermore, examples of practical designs in other technologies, including MMIC, acoustic wave, multilayer, substrate-integrated cavity, and waveguide realizations, are also presented.

Multiband BPFs

Compared to their single-band BPF counterparts, the development of reflectionless multiband BPF components is a more challenging task, as corroborated by the very few examples of absorptive multiband BPF devices reported to date in the technical literature [32], [38]–[40]. This is because, in this case, the out-of-band RF signal power absorption action must be carried out in a higher number of relatively wide nonfrequency-contiguous stopband intervals, separated by the different transmission bands of the multiband BPF (i.e., $N + 1$ stopband regions for an N-band BPF architecture). Furthermore, the influence of the resistive network for the out-of-band RF signal power absorption in the passband ranges must be as transparent as possible to avoid deteriorating the in-band amplitude flatness and producing additional insertion loss. Such design difficulties can be understood either from a theoretical or a practical perspective, depending on the specific technique and microwave technology adopted for the reflectionless multiband BPF realization.

As the most obvious approach, it is well known that several classes of single-to-multiband frequency mappings have been proposed to transform a lossless single-band BPF network to an associated multiband BPF scheme, which preserves the kind of filtering profile (e.g., the Butterworth, Chebyshev, and quasi-elliptic

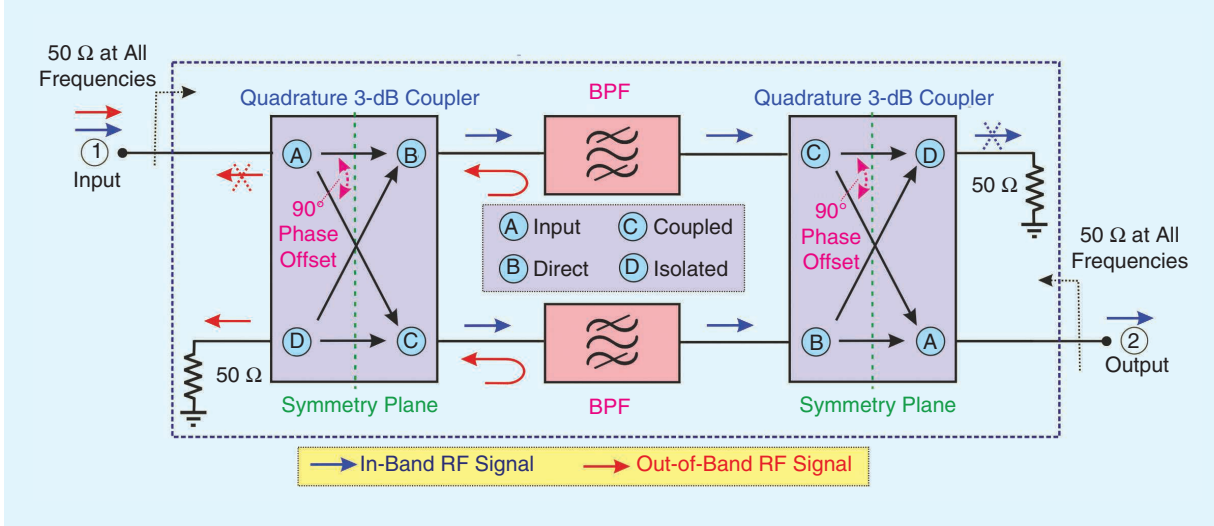

Figure 4. *The conceptual block diagram and operational principle of a two-port reflectionless BPF based on a balanced circuit architecture [33], [34].*

types) for all transmission bands [41], [42]. Such frequency transformations can be equally applied to lossy reflectionless BPF networks to implement absorptive multiband BPFs with an arbitrary number of transmission bands. One example of such a procedure is described in [38] for the design of an input reflectionless dual-band BPF based on a split-type, single-to-dual-band frequency transformation and a complementary diplexer structure.

Specifically, by transforming the inline resonators in the main bandpass and auxiliary bandstop branches of the complementary diplexer network into tree-shaped configurations with three resonating nodes, a dual-band transfer function with the simultaneous inhibition of out-of-band RF signal power transmission and reflection at the input terminal is obtained. This is illustrated in Figure 6(a) for a microstrip transmission line prototype with second-order dual passbands centered at 3.85 and 4.55 GHz, which also exhibits close-to-passband TZs. However, a major limitation of this technique can be found in the reflectionless bandwidth reduction associated with the frequency dependence of the transmission line-based impedance inverters, which becomes more prominent as more inverters are needed in the dual-band BPF network. It should also be noted that, inspired by this complementary diplexer scheme, other dual-band BPF architectures have been proposed, such as the one in [39], which utilizes quasi-complementary broadband, dual-passband, and dual-stopband signal interference filters in the main and

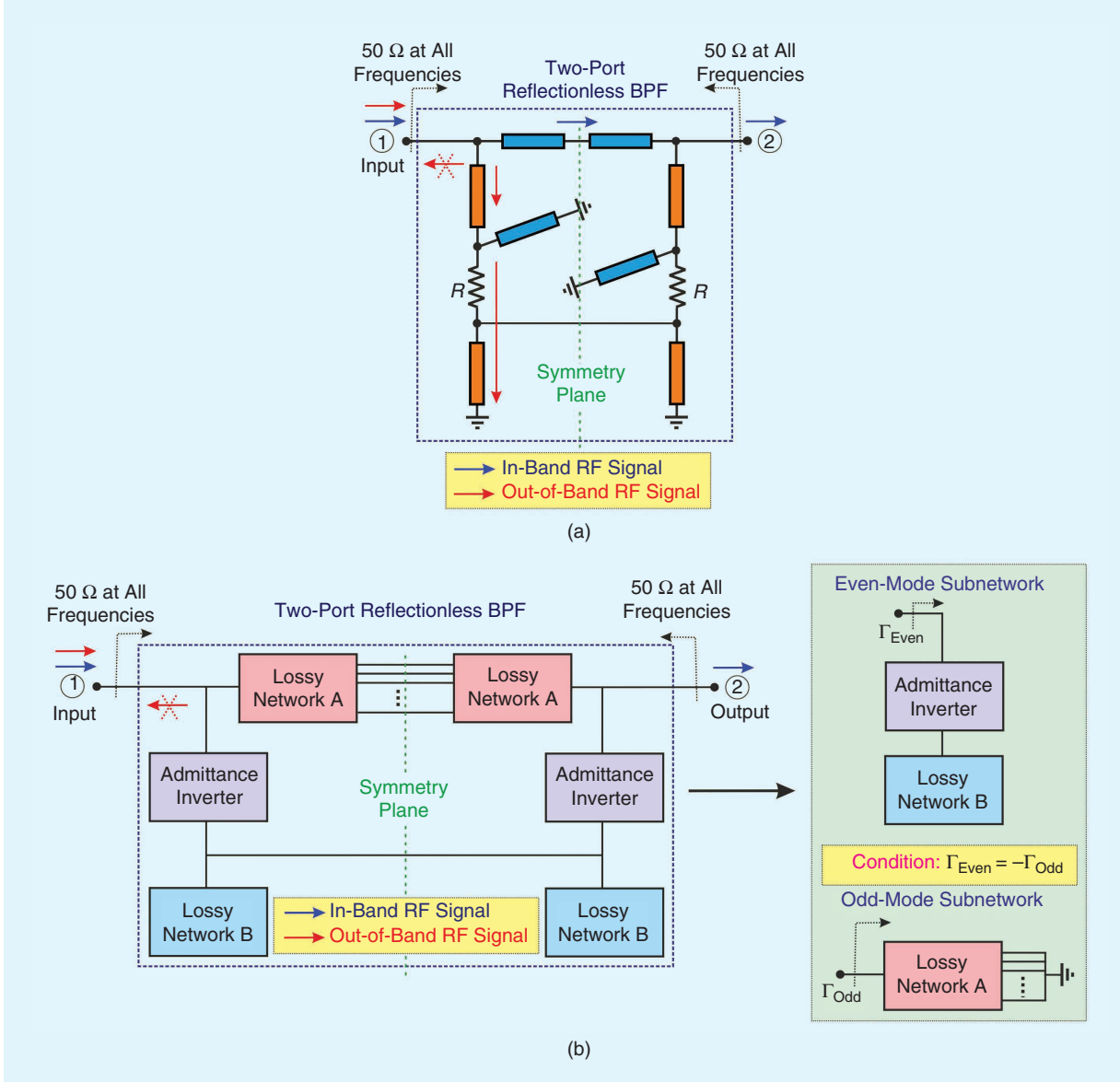

Figure 5. *Two-port reflectionless BPFs. (a) The transmission line design in [35]. (b) The generic approach in [37].*

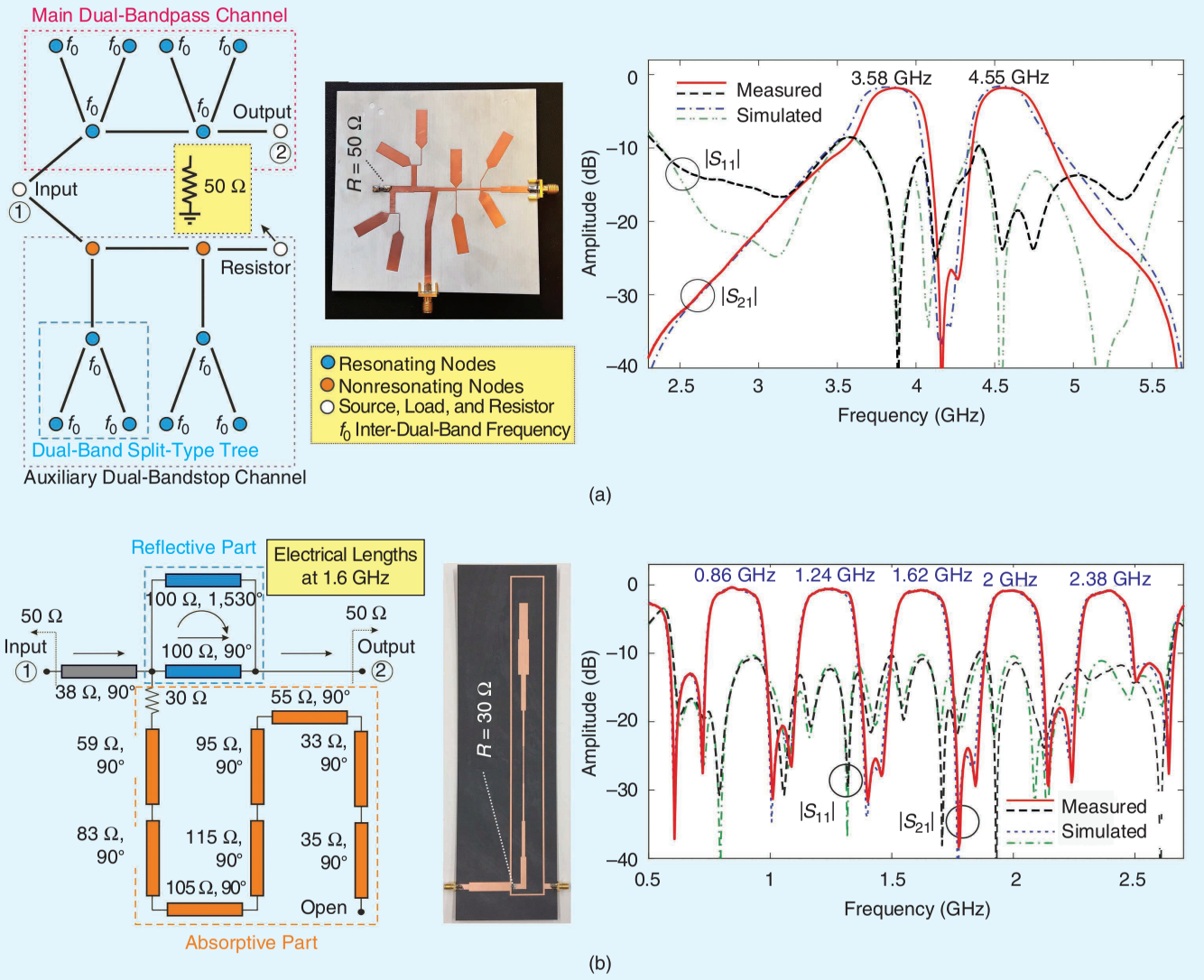

Figure 6. *Examples of input reflectionless, multiband BPFs in microstrip technology. (a) A dual-band BPF based on a split-type complementary diplexer architecture [38]. (b) A five-band BPF based on a lossy transversal signal-interference filtering section [32].*

auxiliary channels to achieve a low RF signal power input reflection.

An alternative philosophy for reflectionless multiband BPF realization exploits modified lossy two-path transversal signal interference filtering sections that have multiband behavior by including absorptive stubs at their input and/or output terminals, shaped by a resistor followed by an open-ended transmission line segment. In this manner, by adequately designing such resistive stubs, a low RF signal power reflection can be attained within the filter stopband regions. The principle is demonstrated in [32] and exemplified in Figure 6(b) for a microstrip prototype corresponding to a 0.86-/1.24-/1.62-/2-/2.38-GHz sharp-rejection five-band BPF by adding only the lossy stub at the input node to attain input reflectionless behavior. The main limitation of this technique is the associated in-band rounding effect produced by the lossy stub across the transmission bands, which slightly deteriorates their amplitude flatness. Nevertheless, as detailed in [8], this shortcoming can be overcome by using more complex (i.e., higher-order) absorptive networks but at the expense of an increased circuit size.

Other procedures have been also applied to multiband reflectionless BPF development, such as the one in [40] that makes use of multimode resonators in a mixed-resistive/transmission line circuit network for a two-port, reflectionless, triple-band BPF design. Whereas such an approach is efficient to attain a wider quasi-reflectionless bandwidth along with triple-band behavior in a compact circuit, its main drawbacks are the lack of theoretical design guidelines and poor reflectionless levels around 5 dB in the passband-to-stopband transitions. Besides, dual-band directional BPFs, as in [43], can be adapted to reflectionless, quasi-elliptic-type dual-band BPFs by loading the output node of the dual-stopband channel with a reference resistor. However, its extension to more-than-two-band designs and closely spaced passbands is not addressed in [43].

Reconfigurable BPFs

The development of reconfigurable microwave filters and multiplexers has become a very popular research topic during the past few years, due to the components' growing importance as the enabling RF hardware for highly versatile next-generation RF transceiver modules capable of ensuring flexible access to the radio resource. In particular, fully adaptive microwave BPFs are highly desired for the dynamic preselection of arbitrary RF signals with different spectral characteristics, whereas reconfigurable BSFs are needed to efficiently mitigate power-/frequency-agile interfering/jamming signals coming from other RF systems operating in the ever-crowded electromagnetic spectrum. As a result, the technical literature on tunable microwave filters is currently quite abundant. Some state-of-the-art candidates for the implementation of controllable single- and multiband BPF components in planar, 3D cavity, and substrate-integrated waveguide technologies that exploit alternative tuning mechanisms can be found in [44]–[47]. Nevertheless, all these microwave filtering devices have a reflective-type nature, hence producing RF signal power reflections in their out-of-band regions for the nontransmitted signals.

Unlike the reflective-type BPF case, the application of RF reconfiguration principles to microwave reflectionless BPF components is just beginning. Indeed, most examples of tunable reflectionless BPF configurations currently available have been engineered during the past five years [24], [48]–[51]. This is true for the ones detailed in [24] and [48], which, respectively, correspond to tunable reflectionless BPFs based on complementary diplexer and absorptive stub solutions. Specifically, in [24], frequency-tunable complementary diplexer networks are proposed for the design of input absorptive microwave BPFs with a tunable center frequency in microstrip and lumped element technologies. In these RF devices, a synchronous tuning process for the resonators of the main bandpass and auxiliary bandstop channels is essential to preserve the input absorptive property for all tunable states.

This technique can also be extrapolated to the development of input reflectionless adaptive multiplexers, as demonstrated in [49], where a single resistively terminated, multistopband filtering branch can be employed as the auxiliary channel to absorb all RF input signal power reflections produced by the bandpass channels in their stopband regions. Figure 7(a) represents the results associated with the mechanically controllable microstrip prototype of the input reflectionless first-order diplexer detailed in [49], which features frequency-tunable lower and upper BPF channels within the spectral range 0.85–1.15 GHz. As can be seen, although the reflectionless behavior is maintained with the reconfiguration process, the passband amplitude asymmetry becomes more significant at the tuning band edges, as the static impedance inverters were designed at the middle frequency of the spectral tuning range.

On the other hand, [48] reports a tunable BPF in terms of the center frequency and bandwidth that employs resonators that can be adjusted in both the resonant frequency and the slope parameter while using a tunable lossy stub at the BPF's input terminal to conduct out-of-band RF signal power absorption. This principle is experimentally verified with a mechanically tunable microstrip prototype of a third-order BPF, in which one major limitation is the passband rounding effect introduced by the controllable lossy

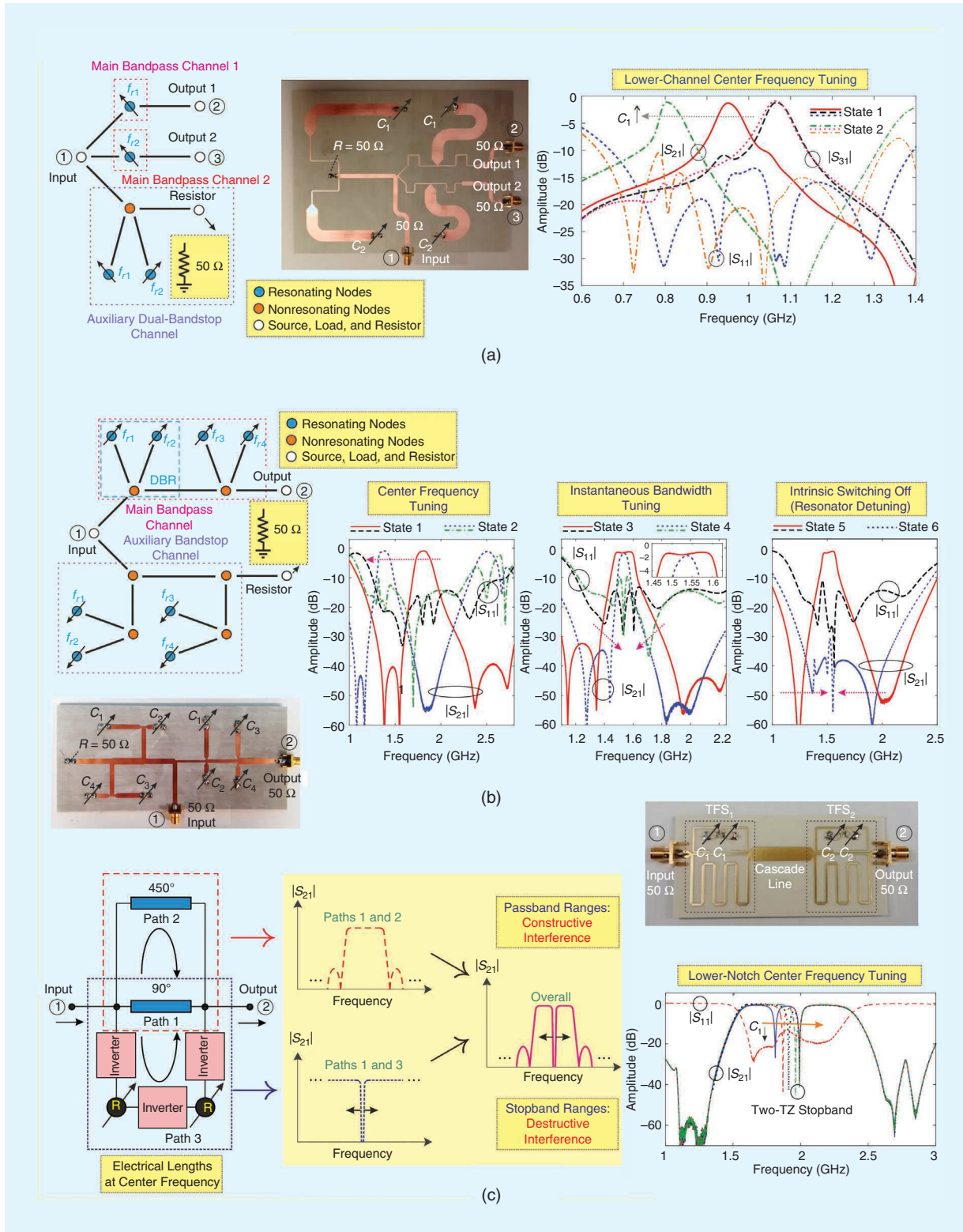

Figure 7. *Examples of reflectionless reconfigurable BPF devices in microstrip technology. (a) An input reflectionless frequency-tunable diplexer based on a complementary diplexer approach [49]. (b) An input reflectionless tune-all BPF based on a complementary diplexer approach [50]. (c) A transversal signal interference wideband BPF with a pair of embedded two-port absorptive notches [51]. TFS: transversal filtering section.*

stub, which becomes more pronounced at the tuning range extremes, as in [24]. Note also that none of these works reports tunable reflectionless BPF circuits with close-to-passband TZs, so their practical usefulness is restricted to low-to-moderate selectivity applications.

As a more advanced input reflectionless BPF component in terms of the number of reconfigurable properties, a tune-all BPF consisting of a dual-behavior resonator (DBR)-based complementary diplexer arrangement is presented in [50]. This architecture is obtained after applying a frequency transformation across the basic input reflectionless BPF scheme in [24] so that each tunable resonating node is converted into an adaptive DBR. Each DBR introduces two TZs below and above its passband when arranged in transmission mode so that a large variety of filtering functionalities can be set through the dynamic reallocation of these TZs.

These capabilities include center frequency agility, bandwidth tuning, amplitude flatness control by positioning the passbands associated with each DBR transfer function at closely spaced center frequencies, and even intrinsic switching-off capabilities (i.e., without the use of RF switches, which results in an in-band lower insertion loss for bandpass states) through the detuning of the resonators in all the DBRs. The input reflectionless behavior can also be ensured for all these selectable modes by synchronously adjusting the DBR resonators in the auxiliary bandstop channel with regard to their peers in the bandpass channel so that a fully adaptive input reflectionless BPF device is obtained. All these reconfiguration capabilities are illustrated in Figure 7(b) for the mechanically tunable proof-of-concept microstrip prototype of the second-order BPF in [50], which can be controlled within the spectral interval of 1.3–2 GHz.

Finally, sharp-rejection wide-passband BPFs, with embedded frequency-agile absorptive notches for the dynamic, reflectionless mitigation of in-band interferers, have also been proposed. This is the case with the microstrip device reported in [51], which makes use of a three-path transversal signal interference filtering section as its building block. Whereas its first and second transmission line paths determine the passband range, the first transmission line path and the third path (made up of impedance inverters and lossy tunable resonators) define the in-band absorptive notch. Thus, by in-series cascading several of these filtering stages, an increased-selectivity broadband filtering action with several embedded tunable notches can be realized. Figure 7(c) depicts the results associated with the microstrip demonstrator in [51] based on two cascaded filtering stages, where the in-band notches can be mechanically tuned and even merged in a single wider and deeper rejection-controllable stopband, within the main passband ranging from 1.6 to 2.4 GHz.

Multifunctional BPF Devices

Due to the necessity of lower-size/volume and optimized RF front ends for emerging wireless systems, the development of RF multifunctional components is currently of great interest [52]–[54]. RF multifunctional components require RF devices capable of carrying out various RF analog signal processing actions in the same circuit volume. The benefits of a multifunctional approach (as opposed to classical RF front-end chains based on an in-series cascade connection of independent monofunctional blocks) include 1) a smaller size, 2) an insertion loss reduction from avoiding interconnecting RF interfaces between separate blocks, and 3) enhanced RF performance by means of the multifunction codesign. Current research efforts focus on integrating the filtering functionality in other types of RF circuits, such as power dividers, amplifiers, and baluns, which results in the conception of completely new families of multioperation filtering devices. Nevertheless, most of these RF components employ a reflective-type filtering, so the availability of reflectionless, multifunctional microwave filtering components is still quite limited.

It should be noted that a reflectionless BPF may be understood as a dual-functional device in and of itself, as it simultaneously provides bandpass filtering and isolatorless impedance matching operations with regard to the reference impedance at theoretically any frequency. Nevertheless, the purpose of this section is to review the very few examples of absorptive BPF devices that have additional cointegrated RF analog signal processing actions.

As the first category, reflectionless BPF/power distribution circuits have been developed, mainly consisting of Wilkinson power dividers and directional couplers with embedded absorptive BPF behavior at some or all ports [55]–[59]. The first example of a reflectionless filtering power divider was reported in [55]; it is based on a complementary diplexer architecture. In this article, a single resistively terminated auxiliary bandstop filtering channel is employed at the input access to absorb the RF signal power reflections coming from the two BPF arms of the power divider. Figure 8(a) illustrates the results corresponding to the reported 2-GHz microstrip proof-of-concept prototype. It shows an input reflectionless second-order BPF capability along with the 3-dB power division action between output nodes, featuring a 2.39:1-ratio bandwidth with a minimum 10-dB power matching level and output isolation levels higher than 13.5 dB in this spectral range. Note that this technique can also be exploited to attain a quasi-reflectionless capability

at both the input and output terminals by loading the absorptive bandstop filtering branch at all ports, as is corroborated in [56].

In [57], using a newly engineered class of lossy isolation networks between output ports that is shaped by two resonators, two resistors, and two impedance inverters, a filtering power divider with reflectionless behavior at its output terminals and wideband interoutput isolation was conceived. However, the developed microstrip prototype shows low-order BPF

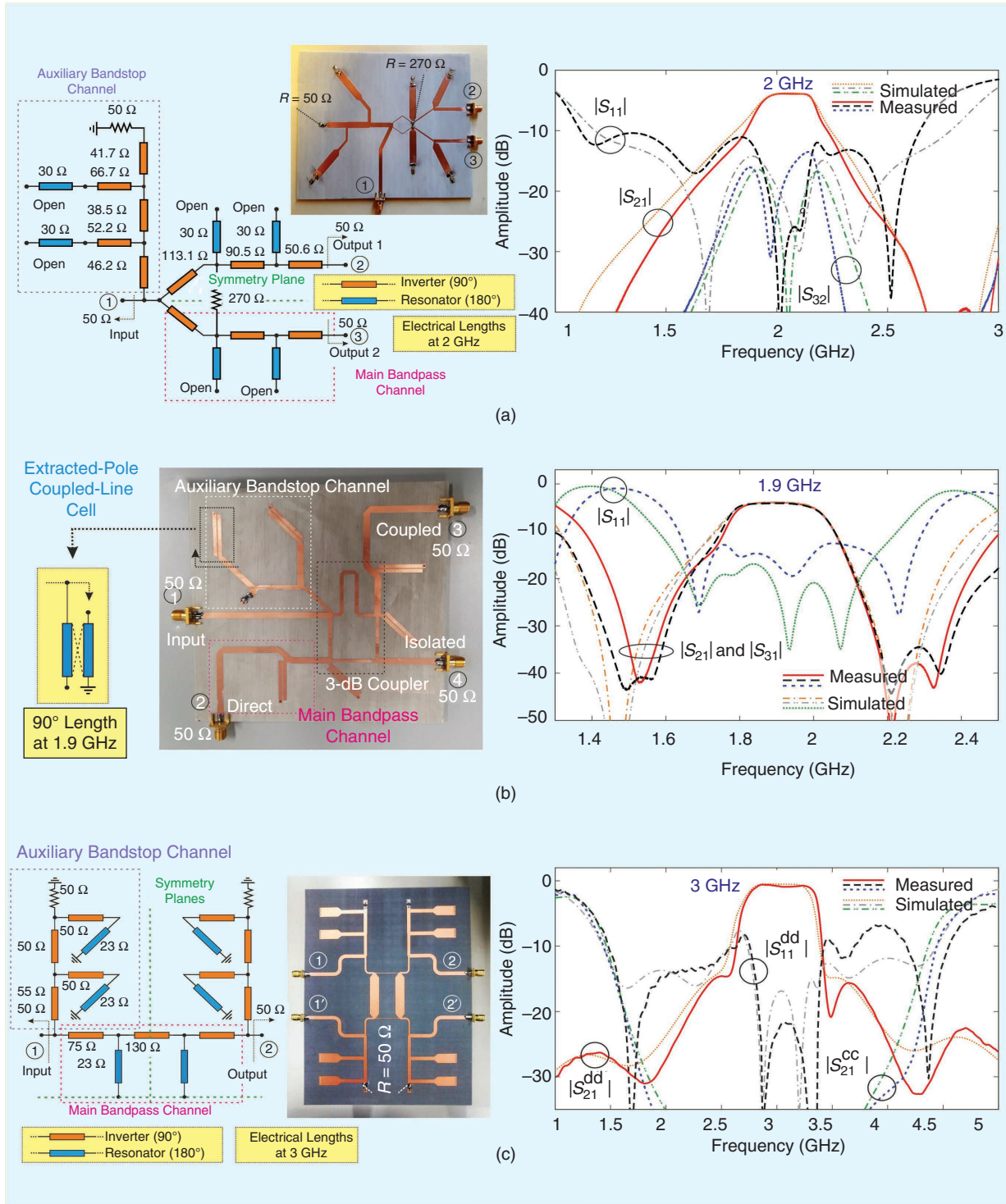

Figure 8. *Examples of reflectionless multifunctional BPF devices based on complementary diplexer approaches in microstrip technology. (a) An input reflectionless filtering power divider [55]. (b) An input reflectionless, out-of-phase, 3-dB filtering coupler [58]. (c) A balanced two-port reflectionless BPF [64].*

behavior, and the extension of this method to attain an all-port reflectionless property is unclear. As an application of the principle in [55] to directional power couplers, an out-of-phase, 3-dB input reflectionless filtering power coupler was proposed in [58]. In this case, second-order BPF channels are embedded in the input-to-direct-port and input-to-coupled-port signal paths, whereas a single complementary bandstop channel is placed at the input access to absorb the out-of-band RF signal energy reflected from both filtering paths.

Figure 8(b) provides the results of the developed microstrip prototype of a 1.9-GHz, second-order demonstrator, in which the input reflectionless bandwidth is reduced with regard to its power divider counterpart, due to the higher frequency dependence of the coupler's 270°-long transmission line segment, which acts as an impedance inverter for the filtering action. A similar concept is used in [59] to implement a 2-GHz quadrature input reflectionless filtering coupler, where multimode resonators and defected ground structures are employed. This approach demonstrates its efficiency in achieving higher circuit compactness and in further extending the input reflectionless stopband bandwidth from dc to 11.5 GHz.

Other examples of dual-function RF components are balanced/differential-mode BPFs, for which a large variety of circuit architectures and design strategies has been proposed during the past few years [60]. These microwave devices mostly exhibit a reflective-type, bandpass-type filtering transfer function in differential-mode operation while inhibiting common-mode RF signal transmission in the differential-mode passband. Such in-band rejection of the common-mode RF signal is generally accomplished through reflection at the balanced input terminal. Other common-mode absorptive BPFs have also been reported, for example, the ones in [61]–[63], where resistors are loaded in the balanced BPF symmetry plane to attain common-mode RF signal energy dissipation.

On the other hand, despite their unquestionable relevance, almost no work has appeared in the literature on the development of balanced BPFs with reflectionless differential-mode characteristics. Indeed, to the best of our knowledge, only the approach in [64] to design two-port absorptive single- and dual-band differential-mode BPFs has been demonstrated. This method adopts the complementary diplexer philosophy at all single-port accesses. Figure 8(c) represents the results corresponding to its 3-GHz microstrip prototype of a second-order balanced BPF, where the in-band, common-mode suppression and the symmetrical reflectionless property are verified.

Finally, it should be noted that simpler multifunctional reflectionless BPF devices have also been proposed, such as the one in [65]. It basically describes an input reflectionless 1.9/2.1-GHz dual-band impedance transformer/BPF circuit, in which the bandpass filtering action can also be viewed as that associated with a dual-band BPF with an arbitrary real-valued load impedance. Furthermore, it must be remarked that the reflectionless philosophy is also capturing the attention of researchers from the antenna community. Examples are absorptive filtering patch antennas with a low RF signal reflection outside the radiation band and reflectionless passive metasurfaces [66], [67].

Other Technologies

The previous sections of this overview article concentrated on reflectionless BPF devices developed in planar realizations. However, although to a much lesser extent, the described RF design principles for absorptive microwave BPFs have also been demonstrated in other technologies. A comprehensive description of the most relevant contributions in the research area of nonplanar, reflectionless BPF components is provided in the following.

- *MMIC and low-frequency technologies [68]–[70]*: Since ferrite-/magnetic-based RF isolators cannot be integrated and active isolator solutions require extra dc power, reflectionless BPFs in MMIC technologies are demanded for modern, energy-efficient, compact RF front-end chains. In [68], using a theoretically perfectly matched symmetrical BPF network with even- and odd-mode subcircuit compensation, an integrated, passive, two-port absorptive BPF is developed. This prototype exhibits a quasi-elliptic-type bandpass filtering response centered at 2.5 GHz with return loss levels above 15 dB from dc to 10 GHz for a chip area of 1 mm^2. It should be noted that commercial counterparts of this solution are already available (X-Series reflectionless filters from Mini-Circuits), showing promise for deployment in future RF transceiver modules. On the other hand, although, thus far, they are used only in low-pass filtering components (which can be easily extended to BPF ones after appropriate low-pass-to-bandpass frequency transformations), the novel classes of reflectionless filters for very-low-frequency applications reported in [69] and [70] can feature generalized filtering transfer function profiles. They are experimentally verified in lumped element technology and avoid the use of negative reactive elements after proper element conversions, which may result from the theoretical synthesis process.
- *Acoustic wave technology [71]*: BPFs in acoustic wave realizations are leading frequency-selective devices in mobile communications systems, due to their high quality factor (Q) and compact footprint

[72]. However, most show some major limitations in terms of their very narrow operational bandwidth and frequency-static filtering transfer function being mostly of the reflective type and because of their spurious mode creation. By efficiently combining the acoustic-wave lumped, element resonator (AWLR) concept presented in [73] for enhanced-bandwidth, quasi-elliptic-type BPF realization with the complementary diplexer approach reported in [24], input reflectionless AWLR-based BPFs with reconfigurable out-of-band TZs are engineered in [71].

Such BPFs have the merits of 1) a bandwidth controllable through the dynamic reallocation of the TZs for values beyond the limit usually imposed by the electromechanical coupling coefficient (k_t^2) of the acoustic wave element, 2) preservation of the high-Q properties inherent in the acoustic wave technology despite the inclusion of the lumped elements, and 3) an input absorptive response. For illustration purposes, Figure 9(a) gives the results of the 418-MHz, second-order proof-of-concept demonstrator built in [71] for one example state, which exhibits an enhanced fractional bandwidth of $1.2k_t^2$, effective Q higher than 6,500, and input reflectionless response with input power matching levels above 15 dB in the represented frequency interval.

- *Multilayer technology [74]*: The exploitation of microstrip-to-microstrip vertical transitions with slot line resonators in multilayer schemes has proven its potential in the development of ultrawideband BPFs aimed at broadband RF receivers [75]. Using this concept and the lossy-stub-loading philosophy for reflectionless BPF design, new ultrawideband BPFs that simultaneously exhibit a very broad, symmetrical, reflectionless behavior can be developed. This is demonstrated in [74], where the employment of multistage input/output lossy stubs to absorb the RF signal power reflections coming from the reflective-type microstrip-to-microstrip vertical-transition component at both accesses enables enhanced-amplitude-flatness, two-port absorptive BPF implementations. Figure 9(b) depicts an example of a multipole proof-of-concept prototype with a fractional bandwidth of roughly 80% near 2 GHz and input/output power matching levels higher than 13.8 dB in the represented spectral band. In addition, this design approach can be applied to the realization of absorptive broadband multifunctional BPF devices, such as input reflectionless filtering baluns [76].
- *Substrate-integrated technology [77]*: With the purpose of achieving reasonably compact physical size/volume, relatively high RF power handling capability, and low in-band insertion loss, substrate-integrated waveguide technology has lately emerged as a tradeoff solution between classic planar and 3D waveguide technologies [78], [79]. Its usefulness in microwave BPF development has been applied not only to the planar integration of conventional waveguide-based BPF schemes but also to evanescent-mode cavity-resonator BPF structures, which enables frequency-adaptive designs using different tuning elements inserted in the cavities, such as microelectromechanical systems, varactors, and piezoelectric actuators [80].

  Recently, in [77], the only example of this type to date, a two-port quasi-reflectionless BPF with substrate-integrated, capacitively loaded coaxial resonators inspired by the symmetrical complementary diplexer approach in [26], was published. It exploits frequency-dependent mixed electromagnetic coupling between the two resonators in the main bandpass channel to attain a two-pole/one-TZ transfer function. Figure 9(c) gives the details and results of the 3.8-GHz proof-of-concept prototype developed in [77], which features 10-dB referred reflectionless bandwidth from 2.9 to 4.9 GHz (i.e., 3.4 times the 3-dB passband width) as the main figure of merit. Obtaining higher values for this quasi-absorptive bandwidth, which is mostly constrained by the particular frequency-dependence profile of the interresonator couplings, remains as a major challenge in this research subject.
- *3D waveguide technology [81], [82]*: BPFs in 3D waveguide implementations are particularly needed in high-RF power-handling and low-loss applications, such as in satellite communication payloads [83]. As such, the availability of reflectionless BPF components developed in this technology is even more necessary, as higher RF signal power reflection levels can be produced, especially on the transmitter side. Despite this, almost no effort has been devoted to the development of reflectionless 3D BPF components. Among the few examples is a millimeter-wave waveguide BPF with an ultrabroad upper stopband through the inhibition of the RF signal transmission at the second and third harmonics [81]. Such harmonic suppression is achieved by means of the RF signal energy absorption properties of a dissipative leaky-wall filtering section, which is combined with a reflective evanescent-mode BPF.

  In this manner, a minimum return loss level of 8 dB is attained from 75 to 140 GHz for a V-band, seven-pole BPF realization. The application of the

complementary diplexer technique to input reflectionless waveguide-cavity BPFs has also been demonstrated in [82]. In this work, an 18-GHz, input reflectionless, quasi-elliptic-type BPF prototype with extracted-pole complementary bandpass and bandstop channels is developed. It shows measured input power matching levels above 20 dB from 17.3 to 18.3 GHz (i.e., 12.5 times the 3-dB bandwidth, equal to 80 MHz), hence verifying the principle.

Finally, note that mixed-technology realizations can also be carried out, where a higher Q technology for the main bandpass channel and a lower Q technology for the auxiliary bandstop channel can be employed while

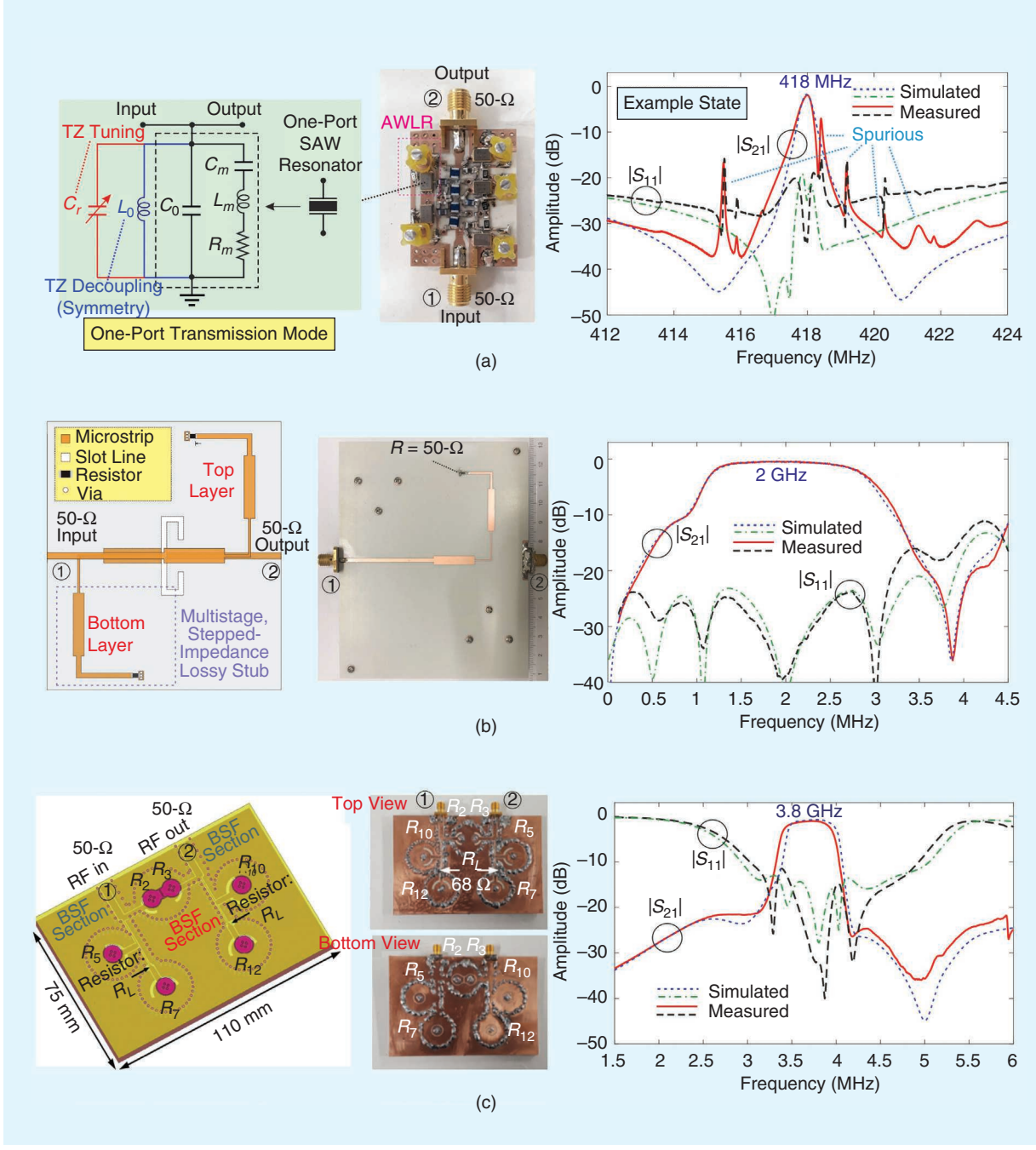

Figure 9. *Examples of reflectionless BPFs in nonplanar technologies. (a) An input reflectionless AWLR-based BPF using a complementary diplexer approach for TZ tuning. [71]. (b) A symmetrical, reflectionless, wideband BPF on multilayer technology using input/output multistage lossy stubs [74]. (c) A symmetrical reflectionless BPF with substrate-integrated coaxial resonators using a two-port complementary diplexer approach [77]. SAW: surface acoustic wave.*

keeping a reasonable level of the higher Q properties in the overall reflectionless BPF. This is the case with the mixed-technology, lumped-element/microstrip, two-port, quasi-reflectionless BPF devices engineered in [84], which are based on symmetrical complementary diplexer arrangements and illustrate this hybrid implementation procedure.

Conclusions

This overview article addressed the emerging topic of reflectionless BPF designs as filtering components that achieve their functionality by means of a frequency-selective RF signal power absorption process inside their lossy circuit structures. As such, the components avoid the creation of out-of-band RF signal power reflections at their access points, which could seriously deteriorate the operation of the earlier active stages in the RF front-end chain (e.g., frequency converters and amplifiers), leading to a complete malfunction. In this manner, they can effectively replace commonly used cascades made up of a conventional reflective-type BPF preceded by an isolator, in the case of active realizations, to absorb the out-of-band RF signal power echoes, which are bulky and difficult to integrate in passive solutions (e.g., magnetic isolators) and which require extra dc power consumption.

Different RF design techniques for microwave reflectionless BPFs were presented, with descriptions of their advantages and drawbacks such as the use of complementary diplexer architectures, input/output lossy stubs, balanced architectures, and networks with intrinsic compensation for their even- and odd-mode subnetworks; these, in some cases, can be viewed as very related approaches. Furthermore, the generalization of these RF design methodologies for reflectionless BPFs to more advanced filtering components, such as absorptive multiband, reconfigurable, and multifunctional BPF devices, was described. Finally, examples of reflectionless BPFs in nonplanar technologies, including MMIC, acoustic wave, multilayer, substrate-integrated cavity, and waveguide realizations, were also discussed. Although some important issues must still be overcome to make these reflectionless BPF devices commercially competitive, such as the influence of the filter absorptive component in the passband region and the robustness to the high temperature levels produced in their lossy elements when dissipating the out-of-band RF signal energy (especially in high-power RF systems), it is clear that these components will play a major role in future isolatorless RF transceivers.

Acknowledgments

This work was supported, in part, by the Spanish Ministry of Economy, Industry, and Competitiveness (State Research Agency), under project TEC2017-82398-R, and by the National Science Foundation, under award 1731956.

References

[1] I. C. Hunter, *Theory and Design of Microwave Filters*. London: IET Press, 2001.

[2] J.-S. Hong, *Microstrip Filters for RF/Microwave Applications*, 2nd ed. Hoboken, NJ: Wiley, 2011.

[3] Mini-Circuits, "Reflectionless filters improve linearity and dynamic range," *Microw. J.*, vol. 58, no. 8, pp. 42–50, Aug. 2015.

[4] M. A. Morgan, "Think outside the band: Design and miniaturization of absorptive filters," *IEEE Microw. Mag.*, vol. 19, no. 7, pp. 54–62, Nov./Dec. 2018. doi: 10.1109/MMM.2018.2862541.

[5] R. Gómez-García, J.-P. Magalhães, J.-M. Muñoz-Ferreras, J. M. N. Vieira, N. B. Carvalho, and J. Pawlan, "Filling the spectral holes: Novel/future wireless communications and radar receiver architectures," *IEEE Microw. Mag.*, vol. 15, no. 2, pp. 45–56, Mar./Apr. 2014. doi: 10.1109/MMM.2013.2296214.

[6] J. D. Adam, "Mitigate the interference: Nonlinear frequency selective ferrite devices," *IEEE Microw. Mag.*, vol. 15, no. 6, pp. 45–56, Sept./Oct. 2014. doi: 10.1109/MMM.2014.2332831.

[7] M. Katanbaf, K.-D. Chu, T. Zhang, C. Su, and J. C. Rudell, "Two-way traffic ahead: RF/analog self-interference cancellation techniques and the challenges for future integrated full-duplex transceivers," *IEEE Microw. Mag.*, vol. 20, no. 2, pp. 22–35, Feb. 2019. doi: 10.1109/MMM.2018.2880489.

[8] M. A. Morgan, *Reflectionless Filters*. Norwood, MA: Artech House, 2017.

[9] D. R. Jachowski, "Compact, frequency-agile, absorptive bandstop filters," in *Proc. IEEE MTT-S Int. Microw. Symp.*, Long Beach, CA, June 11–17, 2005, pp. 513–516. doi: 10.1109/MWSYM.2005.1516645.

[10] A. C. Guyette, I. C. Hunter, R. D. Pollard, and D. R. Jachowski, "Perfectly-matched bandstop filters using lossy resonators," in *Proc. IEEE MTT-S Int. Microw. Symp.*, Long Beach, CA, June 11–17, 2005, pp. 517–520. doi: 10.1109/MWSYM.2005.1516646.

[11] T. Snow, J. Lee, and W. J. Chappell, "Tunable high quality-factor absorptive bandstop filter design," in *Proc. IEEE MTT-S Int. Microw. Symp. Dig.*, Montréal, QC, June 17–22, 2012, pp. 1–3. doi: 10.1109/MWSYM.2012.6259759.

[12] D. Psychogiou, R. Mao, and D. Peroulis, "Series-cascaded absorptive notch-filters for 4G-LTE radios," in *Proc. IEEE Radio Wireless Symp.*, San Diego, CA, Jan. 25–28, 2015, pp. 177–179. doi: 10.1109/RWS.2015.7129726.

[13] J.-Y. Shao and Y.-S. Lin, "Narrowband coupled-line bandstop filter with absorptive stopband," *IEEE Trans. Microw. Theory Techn.*, vol. 63, no. 10, pp. 3469–3478, Oct. 2015. doi: 10.1109/TMTT.2015.2460752.

[14] T.-H. Lee, B. Kim, K. Lee, W. J. Chappell, and J. Lee, "Frequency-tunable low-Q lumped-element resonator bandstop filter with high attenuation," *IEEE Trans. Microw. Theory Techn.*, vol. 64, no. 11, pp. 3549–3556, Nov. 2016. doi: 10.1109/TMTT.2016.2604318.

[15] S.-H. Chien and Y.-S. Lin, "Novel wideband absorptive bandstop filters with good selectivity," *IEEE Access*, vol. 5, pp. 18,847–18,861, Sept. 2017. doi: 10.1109/ACCESS.2017.2752903.

[16] R. Gómez-García, J.-M. Muñoz-Ferreras, and D. Psychogiou, "Symmetrical quasi-reflectionless BSFs," *IEEE Microw. Wireless Compon. Lett.*, vol. 28, no. 4, pp. 302–304, Apr. 2018. doi: 10.1109/LMWC.2018.2805462.

[17] M. Hickle and D. Peroulis, "Theory and design of frequency-tunable absorptive bandstop filters," *IEEE Trans. Circuits Syst. I, Reg. Papers*, vol. 65, no. 6, pp. 1862–1874, June 2018. doi: 10.1109/TCSI.2017.2766206.

[18] M. Kong, Y. Wu, Z. Zhuang, Y. Liu, and A. A. Kishk, "Compact wideband reflective/absorptive bandstop filter with multitransmission zeros," *IEEE Trans. Microw. Theory Techn.*, vol. 67, no. 2, pp. 482–493, Feb. 2019. doi: 10.1109/TMTT.2018.2886847.

[19] R. Gómez-García, L. Yang, J.-M. Muñoz-Ferreras, and W. Feng, "Lossy signal-interference filters and applications," *IEEE Trans.*

Microw. Theory Techn., vol. 68, no. 2, pp. 516–529, Feb. 2020. doi: 10.1109/TMTT.2019.2953585.

[20] Y. Morimoto et al., "A multiharmonic absorption circuit using quasi-multilayered striplines for RF power amplifiers," *IEEE Trans. Microw. Theory Techn.*, vol. 65, no. 1, pp. 109–118, Jan. 2017. doi: 10.1109/TMTT.2016.2614929.

[21] R. Gómez-García, J.-M. Muñoz-Ferreras, W. Feng, and D. Psychogiou, "Input-reflectionless negative-group-delay bandstop-filter networks based on lossy complementary duplexers," in *Proc. 2019 IEEE MTT-S Int. Microw. Symp.*, Boston, MA, June 2–7, 2019, pp. 1031–1034. doi: 10.1109/MWSYM.2019.8700887.

[22] J. Lee and J. Lee, "Distributed-element reflectionless bandstop filter with a broadband impedance matching," *IEEE Microw. Wireless Compon. Lett.*, vol. 30, no. 6, pp. 561–564, 2020. doi: 10.1109/LMWC.2020.2990986.

[23] M.-Á. Sánchez-Soriano, Y. Queré, V. L. Saux, C. Quendo, and S. Cadiou, "Average power handling capability of microstrip passive circuits considering metal housing and environment conditions," *IEEE Trans. Compon., Packag., Manuf. Technol.*, vol. 4, no. 10, pp. 1624–1633, Oct. 2015. doi: 10.1109/TCPMT.2014.2345100.

[24] D. Psychogiou and R. Gómez-García, "Reflectionless adaptive RF filters: Bandpass, bandstop, and cascade designs," *IEEE Trans. Microw. Theory Techn.*, vol. 65, no. 11, pp. 4593–4605, Nov. 2017. doi: 10.1109/TMTT.2017.2734086.

[25] R. Gómez-García, J.-M. Muñoz-Ferreras, and D. Psychogiou, "High-order input-reflectionless bandpass/bandstop filters and multiplexers," *IEEE Trans. Microw. Theory Techn.*, vol. 67, no. 9, pp. 3683–3695, Sept. 2019. doi: 10.1109/TMTT.2019.2924975.

[26] R. Gómez-García, J.-M. Muñoz-Ferreras, and D. Psychogiou, "Symmetrical quasi-absorptive RF bandpass filters," *IEEE Trans. Microw. Theory Techn.*, vol. 67, no. 4, pp. 1472–1482, Apr. 2019. doi: 10.1109/TMTT.2019.2895531.

[27] C. Luo et al., "Quasi-reflectionless microstrip bandpass filters using bandstop filter for out-of-band improvement," *IEEE Trans. Circuits Syst. II, Exp. Briefs*, vol. 67, no. 10, pp. 1849–1853, Oct. 2020. doi: 10.1109/TCSII.2019.2946915.

[28] C. Liu, Z. Deng, X. Liu, and X. Luo, "A wideband bandpass filter with broad stopband and ultra-wide reflectionless range for 5G applications," in *Proc. IEEE MTT-S Int. Microw. Symp. Dig.*, Boston, MA, June 2–7, 2019, pp. 834–837. doi: 10.1109/MWSYM.2019.8700856.

[29] S. W. Jeong, T.-H. Lee, and J. Lee, "Absorptive filter prototype and distributed-element absorptive bandpass filter," in *Proc. 2018 IEEE MTT-S Int. Conf. Numer. Electromagn. Multiphys. Model. Optim.*, Reykjavik, Iceland, Aug. 8–10, 2018, pp. 1–4. doi: 10.1109/NEMO.2018.8503135.

[30] T.-H. Lee, B. Lee, Y.-S. Kim, K. Wu, and J. Lee, "Higher order lumped element low-pass and bandpass filters structures," *IET Microw., Antennas Propag.*, vol. 13, no. 8, pp. 1166–1173, July 2019. doi: 10.1049/iet-map.2018.5479.

[31] X. Wu, Y. Li, and X. Liu, "High-order dual-port quasi-absorptive microstrip coupled-line bandpass filters," *IEEE Trans. Microw. Theory Techn.*, vol. 68, no. 4, pp. 1462–1475, Apr. 2020. doi: 10.1109/TMTT.2019.2955692.

[32] R. Gómez-García, L. Yang, and J.-M. Muñoz-Ferreras, "Low-reflection signal-interference single- and multipassband filters with shunted lossy stubs," *IEEE Microw. Wireless Compon. Lett.*, vol. 30, no. 4, pp. 355–358, Apr. 2020. doi: 10.1109/LMWC.2020.2977864.

[33] A. C. Guyette, I. C. Hunter, and R. D. Pollard, "Design of absorptive microwave filters using allpass networks in a parallel-cascade configuration," in *Proc. IEEE MTT-S Int. Microw. Symp.*, Boston, MA, June 7–12, 2009, pp. 733–736. doi: 10.1109/MWSYM.2009.5165801.

[34] P. Ma, B. Wei, Y. Heng, C. Luo, X. Guo, and B. Cao, "Design of absorptive superconducting filter," *Electron. Lett.*, vol. 53, no. 11, pp. 728–730, May 2017. doi: 10.1049/el.2017.0768.

[35] M. A. Morgan and T. A. Boyd, "Theoretical and experimental study of a new class of reflectionless filter," *IEEE Trans. Microw. Theory Techn.*, vol. 59, no. 5, pp. 1214–1221, May 2011. doi: 10.1109/TMTT.2011.2113189.

[36] M. Khalaj-Amirhosseini and M.-M. Taskhiri, "Twofold reflectionless filters of inverse-Chebyshev response with arbitrary attenuation," *IEEE Trans. Microw. Theory Techn.*, vol. 65, no. 11, pp. 4616–4620, Nov. 2017. doi: 10.1109/TMTT.2017.2716940.

[37] J. Lee, B. Lee, S. Nam, and J. Lee, "Rigorous design method for symmetric reflectionless filters with arbitrary prescribed transmission response," *IEEE Trans. Microw. Theory Techn.*, vol. 68, no. 6, pp. 2300–2307, 2020. doi: 10.1109/TMTT.2020.2976967.

[38] R. Gómez-García, J.-M. Muñoz-Ferreras, and D. Psychogiou, "Split-type input-reflectionless multiband filters," *IEEE Microw. Wireless Compon. Lett.*, vol. 28, no. 11, pp. 981–983, Nov. 2018. doi: 10.1109/LMWC.2018.2868091.

[39] R. Gómez-García, J.-M. Muñoz-Ferreras, W. Feng, and D. Psychogiou, "Wide-band signal-interference duplexer with contiguous single/dual-band channels and its application to quasi-absorptive bandpass filters," *Electron. Lett.*, vol. 54, no. 9, pp. 578–580, May 2018. doi: 10.1049/el.2018.0503.

[40] Z. Cao, X. Bi, and Q. Xu, "Reflectionless triple-band BPF by reused even-mode resonances of multi-mode resonator," *Electron. Lett.*, vol. 55, no. 10, pp. 609–611, May 2019. doi: 10.1049/el.2019.0439.

[41] G. Macchiarella and S. Tamiazzo, "Design techniques for dual-passband filters," *IEEE Trans. Microw. Theory Techn.*, vol. 53, no. 11, pp. 3265–3271, Nov. 2005. doi: 10.1109/TMTT.2005.855749.

[42] A. García-Lampérez and M. Salazar-Palma, "Single-band to multiband frequency transformation for multiband filters," *IEEE Trans. Microw. Theory Techn.*, vol. 59, no. 12, pp. 3048–3058, Dec. 2011. doi: 10.1109/TMTT.2011.2170579.

[43] H. Lobato-Morales, A. Corona-Chávez, T. Itoh, and J. L. Olvera-Cervantes, "Dual-band multi-pole directional filter for microwave multiplexing applications," *IEEE Microw. Wireless Compon. Lett.*, vol. 21, no. 12, pp. 643–645, Dec. 2012. doi: 10.1109/LMWC.2011.2172683.

[44] J.-S. Hong, "Reconfigurable planar filters," *IEEE Microw. Mag.*, vol. 10, no. 6, pp. 73–83, Oct. 2009. doi: 10.1109/MMM.2009.933590.

[45] R. R. Mansour, "High-Q tunable dielectric resonator filters," *IEEE Microw. Mag.*, vol. 10, no. 6, pp. 84–98, June 2009. doi: 10.1109/MMM.2009.933591.

[46] D. Psychogiou, R. Gómez-García, and D. Peroulis, "Recent advances in reconfigurable microwave filter design," in *Proc. 2016 IEEE Wireless Microw. Technol. Conf.*, Clearwater Beach, FL, Apr. 11–13, 2016, pp. 1–6. doi: 10.1109/WAMICON.2016.7483863.

[47] J. D. Martínez, S. Sirci, V. E. Boria, and M. A. Sánchez-Soriano, "When compactness meets flexibility: Basic coaxial SIW filter topology for device miniaturization, design flexibility, advanced filtering responses, and implementation of tunable filters," *IEEE Microw. Mag.*, vol. 21, no. 6, pp. 58–78, June 2020. doi: 10.1109/MMM.2020.2979155.

[48] S.-W. Jeong, T.-H. Lee, and J. Lee, "Frequency- and bandwidth-tunable absorptive bandpass filter," *IEEE Trans. Microw. Theory Techn.*, vol. 67, no. 6, pp. 2172–2180, June 2019. doi: 10.1109/TMTT.2019.2914111.

[49] R. Gómez-García, J.-M. Muñoz-Ferreras, and D. Psychogiou, "Tunable input-quasi-reflectionless multiplexers," in *Proc. 2018 IEEE MTT-S Int. Microw. Workshop Ser. 5G Hardware Syst. Technol.*, Dublin, Ireland, Aug. 30–31, 2018, pp. 1–3. doi: 10.1109/IMWS-5G.2018.8484353.

[50] R. Gómez-García, J.-M. Muñoz-Ferreras, and D. Psychogiou, "Dual-behavior resonator-based fully-reconfigurable input reflectionless bandpass filters," *IEEE Microw. Wireless Compon. Lett.*, vol. 29, no. 1, pp. 35–37, Jan. 2019. doi: 10.1109/LMWC.2018.2884151.

[51] D. Psychogiou, R. Gómez-García, and D. Peroulis, "Wide-passband filters with in-band tunable notches for agile multi-interference suppression in broad-band antenna systems," in *Proc. 2018 IEEE Radio Wireless Symp.*, Anaheim, CA, Jan. 14–17, 2018, pp. 213–216. doi: 10.1109/RWS.2018.8304990.

[52] N. Yang, C. Caloz, and K. Wu, "Greater than the sum of its parts," *IEEE Microw. Mag.*, vol. 11, no. 4, pp. 69–82, June 2010. doi: 10.1109/MMM.2010.936495.

[53] R. Gómez-García, D. Psychogiou, and D. Peroulis, "Single/multi-band multi-functional passive components with reconfiguration capabilities," in *Proc. 2017 IEEE Radio Wireless Symp.*, Phoenix, AZ, Jan. 15–18, 2017, pp. 9–12. doi: 10.1109/RWS.2017.7885930.

[54] X. Y. Zhang and J.-X. Xu, "Multifunctional filtering circuits: 3D multifunctional filtering circuits based on high-Q dielectric resonators and coaxial resonators," *IEEE Microw. Mag.*, vol. 21, no. 3, pp. 50–68, Mar. 2020. doi: 10.1109/MMM.2019.2958164.

[55] R. Gómez-García, J.-M. Muñoz-Ferreras, and D. Psychogiou, "RF reflectionless filtering power dividers," *IEEE Trans. Circuits Syst. II, Exp. Briefs*, vol. 66, no. 6, pp. 933–937, June 2019. doi: 10.1109/TCSII.2018.2875172.

[56] R. Gómez-García, J.-M. Muñoz-Ferreras, and D. Psychogiou, "3-dB filtering power dividers with quasi-reflectionless behavior at all their ports," in *Proc. IEEE MTT-S Int. Microw. Workshop Adv. Mater. Process.*, Bochum, Germany, July 16–18, 2019, pp. 73–75. doi: 10.1109/IMWS-AMP.2019.8880092.

[57] B. Lee, S. Nam, and J. Lee, "Filtering power divider with reflectionless response and wide isolation at output ports," *IEEE Trans. Microw. Theory Techn.*, vol. 67, no. 7, pp. 2684–2692, July 2019. doi: 10.1109/TMTT.2019.2913650.

[58] R. Gómez-García, L. Yang, J.-M. Muñoz-Ferreras, and D. Psychogiou, "Single/multi-band coupled-multi-line filtering section and its application to RF diplexers, bandpass/bandstop filters, and filtering couplers," *IEEE Trans. Microw. Theory Techn.*, vol. 67, no. 10, pp. 3959–3972, Oct. 2019. doi: 10.1109/TMTT.2019.2933212.

[59] W. Yu, Y. Rao, H. J. Qian, and X. Luo, "Reflectionless filtering 90° coupler using stacked cross coupled-line and loaded cross-stub," *IEEE Microw. Wireless Compon. Lett.*, vol. 30, no. 5, pp. 481–484, May 2020. doi: 10.1109/LMWC.2020.2986155.

[60] F. Martin, L. Zhu, J.-S. Hong, and F. Medina, *Balanced Microwave Filters*, 1st ed. Hoboken, NJ: Wiley, 2018.

[61] W. Zhang, Y. Wu, Y. Liu, C. Yu, A. Hasan, and F. M. Ghannouchi, "Planar wideband differential-mode bandpass filter with common-mode noise absorption," *IEEE Microw. Wireless Compon. Lett.*, vol. 27, no. 5, pp. 458–460, May 2017. doi: 10.1109/LMWC.2017.2690839.

[62] Y. Zhu, K. Song, M. Fan, S. Guo, Y. Zhou, and Y. Fan, "Wideband balanced bandpass filter with common-mode noise absorption using double-sided parallel-strip line," *IEEE Microw. Wireless Compon. Lett.*, vol. 30, no. 4, pp. 359–362, Apr. 2020. doi: 10.1109/LMWC.2020.2974089.

[63] Y. Guan, Y. Wu, and M. M. Tentzeris, "A bidirectional absorptive common-mode filter based on interdigitated microstrip coupled lines for 5G "Green" communications," *IEEE Access*, vol. 8, no. 4, pp. 20,759–20,769, 2020. doi: 10.1109/ACCESS.2020.2968931.

[64] R. Gómez-García, J.-M. Muñoz-Ferreras, W. Feng, and D. Psychogiou, "Balanced symmetrical quasi-reflectionless single- and dual-band bandpass planar filters," *IEEE Microw. Wireless Compon. Lett.*, vol. 28, no. 9, pp. 798–800, Sept. 2018. doi: 10.1109/LMWC.2018.2856400.

[65] R. Gómez-García, J.-M. Muñoz-Ferreras, and D. Psychogiou, "Multi-band reflectionless filtering impedance transformers," in *Proc. 2018 IEEE Int. Wireless Symp.*, Chengdu, China, May 6–10, 2018, pp. 1–4. doi: 10.1109/IEEE-IWS.2018.8400798.

[66] Y.-T. Liu, K. W. Leung, and N. Yang, "Compact absorptive filtering patch antenna," *IEEE Trans. Antennas Propag.*, vol. 68, no. 2, pp. 633–642, Feb. 2020. doi: 10.1109/TAP.2019.2938798.

[67] B. O. Zhu and Y. Feng, "Passive metasurface for reflectionless and arbitrary control of electromagnetic wave transmission," *IEEE Trans. Antennas Propag.*, vol. 63, no. 12, pp. 5500–5511, Dec. 2015. doi: 10.1109/TAP.2015.2481479.

[68] M. A. Morgan and T. A. Boyd, "Reflectionless filter structures," *IEEE Trans. Microw. Theory Techn.*, vol. 63, no. 4, pp. 1263–1271, Apr. 2015. doi: 10.1109/TMTT.2015.2403841.

[69] M. A. Morgan, W. M. Groves, and T. A. Boyd, "Reflectionless filter topologies supporting arbitrary low-pass ladder prototypes," *IEEE Trans. Circuits Syst. I, Reg. Papers*, vol. 66, no. 2, pp. 594–604, Feb. 2019. doi: 10.1109/TCSI.2018.2872424.

[70] A. Guilabert, M. A. Morgan, and T. A. Boyd, "Reflectionless filters for generalized elliptic transmission functions," *IEEE Trans. Circuits Syst. I, Reg. Papers*, vol. 66, no. 12, pp. 4606–4618, Dec. 2019. doi: 10.1109/TCSI.2019.2931469.

[71] D. Psychogiou and R. Gómez-García, "Symmetrical quasi-reflectionless SAW-based bandpass filters with tunable bandwidth," *IEEE Microw. Wireless Compon. Lett.*, vol. 29, no. 7, pp. 447–449, July 2019. doi: 10.1109/LMWC.2019.2918413.

[72] A. Hagelauer, G. Fattinger, C. C. W. Ruppel, M. Ueda, K.-y. Hashimoto, and A. Tag, "Microwave acoustic wave devices: Recent advances on architectures, modeling, materials, and packaging," *IEEE Trans. Microw. Theory Techn.*, vol. 66, no. 10, pp. 4548–4562, Oct. 2018. doi: 10.1109/TMTT.2018.2854160.

[73] D. Psychogiou, R. Gómez-García, R. Loeches-Sánchez, and D. Peroulis, "Hybrid acoustic-wave-lumped-element resonators (AWLRs) for high-Q bandpass filters with quasi-elliptic frequency response," *IEEE Trans. Microw. Theory Techn.*, vol. 63, no. 7, pp. 2233–2244, July 2015. doi: 10.1109/TMTT.2015.2438894.

[74] L. Yang, R. Gómez-García, J.-M. Muñoz-Ferreras, R. Zhang, D. Peroulis, and L. Zhu, "Multilayered reflectionless wideband bandpass filters with shunt/in-series resistively-terminated microstrip lines," *IEEE Trans. Microw. Theory Techn.*, vol. 68, no. 3, pp. 877–893, Mar. 2020. doi: 10.1109/TMTT.2019.2952861.

[75] L. Yang et al., "Novel multilayered ultra-broadband bandpass filters on high-impedance slotline resonators," *IEEE Trans. Microw. Theory Techn.*, vol. 67, no. 1, pp. 129–139, Jan. 2019. doi: 10.1109/TMTT.2018.2873330.

[76] L. Yang, R. Gómez-García, J.-M. Muñoz-Ferreras, and W. Feng, "Multilayered wideband balun bandpass filters designed with input-reflectionless response," in *Proc. 49th Eur. Microw. Conf.*, Paris, France, Oct. 1–3, 2019, pp. 452–455. doi: 10.23919/EuMC.2019.8910806.

[77] D. Psychogiou and R. Gómez-García, "Quasi-absorptive substrate-integrated bandpass filters using capacitively-loaded coaxial resonators," in *Proc. IEEE MTT-S Int. Microw. Symp.*, Los Angeles, CA, Aug. 2020, pp. 663–666.

[78] X. P. Chen and K. Wu, "Substrate integrated waveguide filters: Practical aspects and design considerations," *IEEE Microw. Mag.*, vol. 15, no. 7, pp. 75–83, 2014. doi: 10.1109/MMM.2014.2355751.

[79] X. P. Chen and K. Wu, "Substrate integrated waveguide filter: Basic design rules and fundamental structure features," *IEEE Microw. Mag.*, vol. 15, no. 5, pp. 108–116, July 2014. doi: 10.1109/MMM.2014.2321263.

[80] D. Peroulis, E. Naglich, M. Sinanis, and M. Hickle, "Tuned to resonance: Transfer-function-adaptive filters in evanescent-mode cavity-resonator technology," *IEEE Microw. Mag.*, vol. 15, no. 5, pp. 55–69, 2014. doi: 10.1109/MMM.2014.2321103.

[81] R. V. Snyder and S. Bastioli, "V-band waveguide bandpass filter with wide stopband and harmonics absorption," in *Proc. 46th Eur. Microw. Conf.*, London, Oct. 4–6, 2016, pp. 245–248. doi: 10.1109/EuMC.2016.7824324.

[82] Y. Yang, M. Yu, X. Yin, and Q. Wu, "On the singly terminated and complementary networks," *IEEE Trans. Microw. Theory Techn.*, vol. 67, no. 3, pp. 988–996, Mar. 2019. doi: 10.1109/TMTT.2019.2894728.

[83] R. J. Cameron, C. M. Kudsia, and R. R. Mansour, *Microwave Filters for Communication Systems: Fundamentals, Design, and Applications*. Hoboken, NJ: Wiley, 2007.

[84] D. J. Simpson, R. Gómez-García, and D. Psychogiou, "Mixed-technology quasi-reflectionless planar filters: Bandpass, bandstop, and multi-band designs," *Int. J. RF Microw. Wireless Technol.*, vol. 11, no. 5–6, pp. 466–474, May/June 2019. doi: 10.1017/S1759078719000230.